

# Microscopic Mechanism of Pair-Density-Wave Superconductivity

Dmitry Miserev, Jelena Klinovaja, and Daniel Loss  
*Department of Physics, University of Basel,  
 Klingelbergstrasse 82, CH-4056 Basel, Switzerland*

(Dated: December 29, 2023)

We present an analytic theory unravelling the microscopic mechanism of high-temperature superconductivity posing a longstanding challenge in condensed matter physics. Our model consists of a  $D$ -dimensional electron gas with electron and hole Fermi surfaces, subject to a repulsive electron-electron interaction of a finite range exceeding the average inter-particle distance. Evaluating susceptibilities in a systematic perturbative approach and via one-loop renormalization group theory, we identify an intrinsic Fermi liquid instability towards the formation of superconducting pair-density-wave order when the interaction coupling strength reaches a universal critical value. Similar singularities in charge and spin susceptibilities at the critical coupling indicate the competition between charge, spin, and pair density wave orders, aligning with the phenomenological understanding of the phase diagram of high-temperature superconductors.

*Introduction.* Strongly correlated phenomena observed in various condensed matter systems have long posed a perplexing challenge to the condensed matter physics community [1–28]. While existing theoretical models have contributed valuable insights into individual phases [29–35], a consensus on the microscopic mechanism underlying high-temperature superconductivity within a realistic model is lacking [1].

A powerful phenomenological description for high-temperature superconductors is based on the pair-density-wave (PDW) origin of superconductivity, which subsequently generates other orders, including charge-density-wave (CDW) order [1, 36–39]. To the best of our knowledge, a microscopic mechanism of the mother PDW state is currently absent [1]. In this paper, we aim to fill this gap and present a general microscopic model that demonstrates the instability of an interacting spin-degenerate electron gas with electron and hole Fermi surfaces, see Fig. 1, towards the PDW superconducting ordering at the critical coupling strength. The interaction is assumed to be a repulsive instantaneous density-density interaction with a finite range  $R_0$  exceeding the inter-particle distance characterized by the Fermi wavelengths. The microscopic mechanism of the PDW formation proposed in this paper lends strong theoretical support to the PDW scenario of superconductivity in cuprate materials [1, 36–39]. We also find similar singularities in the  $2k_e$  and  $2k_h$  harmonics of the intra-pocket charge and spin susceptibilities, where  $k_e$  and  $k_h$  are the Fermi momenta of the electron and the hole pocket, respectively, see Fig. 1. These singularities signal a competition between PDW, CDW, and spin-density-wave (SDW) orders, which is also consistent with experimental observations in cuprate materials [2–9].

In the single-pocket model with a repulsive finite-range interaction, singularities at the critical coupling are identified exclusively in the  $2k_F$  harmonics of charge and spin susceptibilities, where  $k_F$  is the Fermi momentum of the pocket. The pair susceptibility remains non-singular at finite momentum. This behavior signals a phase transi-

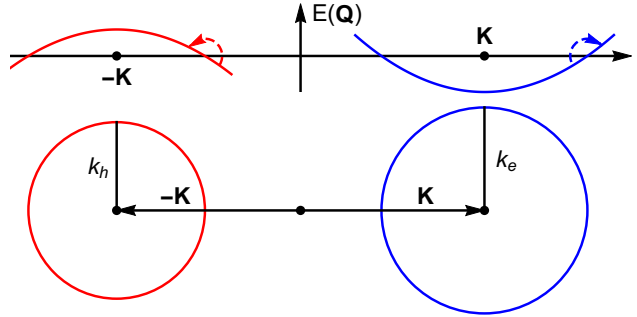


FIG. 1. **Particle spectrum and Fermi surfaces.**  $D$ -dimensional, spin degenerate, electron (blue) and hole (red) Fermi pockets with the Fermi momenta  $k_e$  and  $k_h$  centered at  $\mathbf{K}$  and  $-\mathbf{K}$ , respectively. The energy vs. momentum  $\mathbf{Q}$ ,  $E(\mathbf{Q})$ , is a sketch of the particle dispersion along the line connecting the centers of the two pockets. Blue and red dashed arrows indicate the inter-pocket scattering process due to repulsive density-density interactions of finite range  $R_0$  responsible for the PDW singularity at finite momentum  $k_e + k_h$ .

tion from the Fermi liquid (FL) to a correlated insulator state characterized by competing CDW and SDW orders. These findings are consistent with metal-to-insulator transitions observed experimentally in ultra-clean semiconductor quantum wells at very low electron densities [10–13].

As the microscopic model considered here is not material-specific, we believe that the mechanism of PDW, CDW, and SDW instabilities described in this work, is also relevant for other strongly correlated electron systems such as magic-angle twisted bilayer and trilayer graphene (MAG) [14–24], bilayer transition metal dichalcogenides [25] and double bilayer graphene [26–28].

Importantly, the repulsive electron-electron interaction within our model is assumed to have a finite range  $R_0$  that significantly exceeds the average inter-electron distance given by the Fermi wavelengths. As it has been recently shown in Ref. [40], such interactions generate large logarithmic corrections to charge and spin suscep-

tibilities already in first-order perturbation theory. In contrast, a short-range (contact) interaction only generates irrelevant non-analyticities [41–43]. Here, we calculate logarithmic corrections to pair, charge, and spin susceptibilities within first and second order perturbation theory, then incorporate them systematically through the renormalization group (RG) procedure [44, 45]. All calculations are performed on the FL side at zero temperature.

*Free susceptibilities.* We consider a zero-temperature, spin-degenerate,  $D$ -dimensional electron gas,  $D > 1$ , with two spherical Fermi surfaces, the electron pocket of radius  $k_e$  centered at momentum  $\mathbf{K}$  and the hole pocket of radius  $k_h$  centered at momentum  $-\mathbf{K}$ , see Fig. 1. The electrons interact via a forward-scattering density-density interaction with a finite range  $R_0$  that is much greater than the inter-particle distance, i.e.  $R_0 \gg \lambda_e = 2\pi/k_e, \lambda_h = 2\pi/k_h$ . The long-distance asymptotics of the free electron,  $G_e(\tau, \mathbf{r})$ , and the free hole,  $G_h(\tau, \mathbf{r})$ , Green's functions at large distances  $r \gg \lambda_e, \lambda_h$  and large imaginary times  $\tau \gg 1/(k_e v_h), 1/(k_h v_e)$ ,  $v_e > 0$  and  $v_h > 0$  are the electron and the hole Fermi velocities, respectively, follows from the general dimensional reduction procedure [46],

$$G_e(\tau, \mathbf{r}) = e^{i\mathbf{K}\cdot\mathbf{r}} \sum_{\nu_e} \frac{e^{i\nu_e(k_e r - \vartheta)}}{(\lambda_e r)^{\frac{D-1}{2}}} g_{\nu_e}(\tau, r), \quad (1)$$

$$G_h(\tau, \mathbf{r}) = e^{-i\mathbf{K}\cdot\mathbf{r}} \sum_{\nu_h} \frac{e^{i\nu_h(k_h r - \vartheta)}}{(\lambda_h r)^{\frac{D-1}{2}}} g_{\nu_h}(\tau, r), \quad (2)$$

where  $\nu_e, \nu_h \in \{\pm 1\}$  are the chiral indices,  $\vartheta = \pi(D-1)/4$  is the semiclassical phase,  $g_{\nu_e}(\tau, x)$  and  $g_{\nu_h}(\tau, x)$  are effective one-dimensional slowly-varying Green's functions,

$$g_{\nu_e}(\tau, x) = \frac{1}{2\pi} \frac{1}{i\nu_e x - v_e \tau}, \quad g_{\nu_h}(\tau, x) = \frac{1}{2\pi} \frac{1}{i\nu_h x + v_h \tau} \quad (3)$$

Note that the hole-like origin of the hole pocket manifests itself in the sign of the  $v_h \tau$  term in  $g_{\nu_h}(\tau, x)$ .

The free static susceptibilities are defined in the standard way,

$$\chi_{P,ab}^{(0)}(\mathbf{r}) = \int_{-\infty}^{\infty} G_a(\tau, \mathbf{r}) G_b(\tau, \mathbf{r}) d\tau, \quad (4)$$

$$\chi_{C/S,ab}^{(0)}(\mathbf{r}) = -2 \int_{-\infty}^{\infty} G_a(\tau, \mathbf{r}) G_b(-\tau, -\mathbf{r}) d\tau, \quad (5)$$

where  $a, b \in \{e, h\}$  and the subscripts  $P$ ,  $C$ , and  $S$  label pair, charge, and spin susceptibilities, respectively. The free charge and spin susceptibilities are the same for a spin-degenerate electron gas, where the factor of 2 in Eq. (5) is due to the spin trace. The intra-pocket pair susceptibilities  $\chi_{P,ee}^{(0)}(\mathbf{r}), \chi_{P,hh}^{(0)}(\mathbf{r})$  have a spin-singlet symmetry, while both spin-singlet and spin-triplet symmetry is possible for the inter-pocket pair susceptibility  $\chi_{P,eh}^{(0)}(\mathbf{r})$ .

The intra-pocket pair susceptibility features  $\mathbf{Q} = \pm 2\mathbf{K}$  long-range harmonics, while the inter-pocket one exhibits the  $Q_{eh}^+ = k_e + k_h$  harmonic,

$$\chi_{P,aa}^{(0)}(\mathbf{r}) = \frac{e^{\pm 2i\mathbf{K}\cdot\mathbf{r}}}{2\pi v_a \lambda_a^{D-1} r^D}, \quad (6)$$

$$\chi_{P,eh}^{(0)}(r) = -\frac{\cos(Q_{eh}^+ r - 2\vartheta)}{\pi(v_e + v_h)(\lambda_e \lambda_h)^{\frac{D-1}{2}} r^D}, \quad (7)$$

where  $a \in \{e, h\}$ , and  $+2\mathbf{K}$  ( $-2\mathbf{K}$ ) in Eq. (6) corresponds to the  $ee$  ( $hh$ ) intra-pocket pair susceptibility. The intra-pocket pair susceptibilities  $\chi_{P,aa}^{(0)}(\mathbf{Q})$  probing the zero-momentum pairing, are logarithmically divergent at  $\mathbf{Q} = \pm 2\mathbf{K}$ , where  $\chi_{P,aa}^{(0)}(\mathbf{Q})$  is the Fourier transform of Eq. (6). Here,  $\mathbf{Q} = \pm 2\mathbf{K}$  is due to the origin choice of the corresponding pocket, see Fig. 1. The Fourier transform  $\chi_{P,eh}^{(0)}(\mathbf{Q})$  of the inter-pocket pair susceptibility in Eq. (7) contains a non-analyticity at  $|\mathbf{Q}| = Q_{eh}^+$  that is not singular at  $D > 1$ . The intra-pocket charge and spin susceptibilities exhibit long-range harmonics at  $|\mathbf{Q}| = 2k_e$  and  $|\mathbf{Q}| = 2k_h$ , while the inter-pocket components oscillate at  $\mathbf{Q} = \pm 2\mathbf{K} + \mathbf{Q}_{eh}^-$ ,  $|\mathbf{Q}_{eh}^-| = Q_{eh}^- = |k_e - k_h|$ ,

$$\chi_{C/S,aa}^{(0)}(r) = \frac{\cos(2k_a r - 2\vartheta)}{\pi v_a \lambda_a^{D-1} r^D}, \quad (8)$$

$$\chi_{C/S,eh}^{(0)}(\mathbf{r}) = -\frac{2e^{2i\mathbf{K}\cdot\mathbf{r}} \cos(Q_{eh}^- r)}{\pi(v_e + v_h)(\lambda_e \lambda_h)^{\frac{D-1}{2}} r^D}, \quad (9)$$

where  $a \in \{e, h\}$  and  $\chi_{C/S,he}^{(0)}(\mathbf{r}) = \chi_{C/S,eh}^{(0)}(-\mathbf{r})$ . In the fine-tuned case of  $k_e = k_h$ , the inter-pocket charge and spin susceptibilities  $\chi_{C/S,eh}^{(0)}(\mathbf{Q}) = \chi_{C/S,he}^{(0)}(-\mathbf{Q})$  diverge logarithmically in momentum space at  $\mathbf{Q} = \pm 2\mathbf{K}$ . Otherwise, the Fourier transforms of the free charge and spin susceptibilities are non-singular at  $D > 1$ .

*First- and second-order interaction corrections.* Next, we consider interaction corrections to the susceptibilities emerging from a repulsive forward-scattering density-density interaction  $U(\tau, \mathbf{r}) = \delta(\tau)V(r)$  of finite range  $R_0 \gg \lambda_e, \lambda_h$ . Following the recipe of calculation used in Ref. [40], which is based on a dimensional reduction technique [46], we find the first-order interaction corrections to the susceptibilities, see the Supplemental Material (SM) [47],

$$\chi_{P,aa}^{(1)}(\mathbf{r}) = -\chi_{P,aa}^{(0)}(\mathbf{r}) \gamma_{aa} \ln\left(\frac{r}{R_0}\right), \quad (10)$$

$$\chi_{P,eh}^{(1)}(r) = \chi_{P,eh}^{(0)}(r) \gamma_{eh} \ln\left(\frac{r}{R_0}\right), \quad (11)$$

$$\chi_{C/S,aa}^{(1)}(r) = \chi_{C/S,aa}^{(0)}(r) \gamma_{aa} \ln\left(\frac{r}{R_0}\right), \quad (12)$$

$$\chi_{C/S,eh}^{(1)}(\mathbf{r}) = -\chi_{C/S,eh}^{(0)}(\mathbf{r}) \gamma_{eh} \ln\left(\frac{r}{R_0}\right), \quad (13)$$

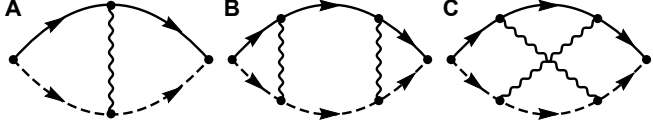


FIG. 2. **Leading logarithmic diagrams for the pair susceptibility in  $D > 1$ .** A: first-order vertex correction; B, C: second-order vertex corrections. The leading logarithmic diagrams for charge and spin susceptibilities share similar structures. Solid (dashed) lines stand for the electron (hole) Green's function, while wavy lines denote the interaction.

where  $a \in \{e, h\}$  and  $r \gg R_0$ . Three dimensionless coupling constants are introduced here,

$$\gamma_{ee} = \frac{2V_2}{\pi v_e}, \quad \gamma_{hh} = \frac{2V_2}{\pi v_h}, \quad \gamma_{eh} = \frac{4V_2}{\pi(v_e + v_h)}. \quad (14)$$

The notation  $V_2$  for the interaction matrix element is inherited from Ref. [40],

$$V_2 = \int_0^\infty V(r) dr \sim \frac{e^2}{\epsilon_\infty}, \quad (15)$$

where  $e$  is the elementary charge and  $\epsilon_\infty$  the dielectric constant. The logarithmic corrections to the susceptibilities originate from vertex corrections, see Fig. 2A, and indicate the emergence of singularities. In case of repulsive interactions ( $\gamma_{ab} > 0$ ), the inter-pocket pair and the intra-pocket charge and spin susceptibilities are logarithmically enhanced, see Eqs. (11), (12), whereas the intra-pocket pair and the inter-pocket charge and spin susceptibilities are suppressed, see Eqs. (10), (13). The situation is opposite for an attractive interaction. In order to construct the one-loop RG, we also require second-order interaction corrections, see Fig. 2B,C.

The second-order Feynman diagrams contributing to  $\log^2$ -corrections of the pair susceptibility are shown in Fig. 2B,C, all other diagrams are subleading in  $D > 1$ , see the SM [47]. It is worth mentioning that at  $D = 1$  there is one more second-order  $\log^2$ -contribution originating from the dynamic screening of the forward-scattering interaction which, however, becomes irrelevant for  $D > 1$ . This constitutes a fundamental difference between  $D = 1$  and  $D > 1$ . Deferring details of the calculations to the SM [47], we provide here only the final results, accurate to leading logarithmic order,

$$\chi_{P/C/S,ab}^{(2)}(\mathbf{r}) = \chi_{P/C/S,ab}^{(0)}(\mathbf{r}) \frac{\gamma_{ab}^2}{2} \ln^2 \left( \frac{r}{R_0} \right), \quad (16)$$

where, again,  $a, b \in \{e, h\}$  and  $r \gg R_0$ .

*Renormalization group.* The sum of diagrams up to second order for each susceptibility takes the following form:

$$\chi(r) = \chi^{(0)}(r) F \left( \frac{r}{R_0}, \gamma_0 \right), \quad (17)$$

$$F(\rho, \gamma_0) = 1 + \gamma_0 \ln \rho + \frac{\gamma_0^2}{2} \ln^2 \rho, \quad (18)$$

where  $\gamma_0 \in \{\pm \gamma_{ab}\}$ ,  $a, b \in \{e, h\}$ , depending on the susceptibility and its harmonic. Here we follow the multiplicative RG approach [44, 45]. Deferring details of the calculations to the SM [47], we find that the susceptibilities are dressed by the power-law form-factor,

$$\chi(r) = \chi^{(0)}(r) \left( \frac{r}{R_0} \right)^{\gamma_0}. \quad (19)$$

Note that the exponentiation of the logarithm is also evident from Eq. (18) as it turns out that the interaction coupling constant does not flow within the one-loop RG (see the SM [47]). The latter fact significantly extends the applicability range of the one-loop RG from the standard scale  $r \lesssim R_0 e^{1/\gamma_0}$  to much larger scales  $r \lesssim R_0 e^{1/\gamma_0^2}$  for  $\gamma_0 \ll 1$ .

*Singularities at  $Q = k_a + k_b$ .* For repulsive interactions [ $\gamma_{ab} > 0$ , see Eq. (14)] only the intra-pocket charge and spin susceptibilities and the inter-pocket pair susceptibility are relevant, all other harmonics are suppressed compared to their non-interacting values. Taking the  $D$ -dimensional Fourier transform, we find the singular behavior of these susceptibilities in momentum space at finite momentum  $k_a + k_b$ ,

$$\chi_{ab}(\delta Q) = \frac{2 \cos \left[ \frac{\pi}{2} \delta \gamma_{ab} + \vartheta \operatorname{sgn}(\delta Q) \right] \Gamma(\delta \gamma_{ab})}{\pi(v_a + v_b) [R_0(\lambda_a + \lambda_b)]^{\gamma_c} |\delta Q R_0|^{\delta \gamma_{ab}}}, \quad (20)$$

$$\gamma_c = \frac{D-1}{2}, \quad (21)$$

where  $\delta \gamma_{ab} = \gamma_{ab} - \gamma_c < 0$ ,  $\delta Q = Q - (k_a + k_b) \ll 1/R_0 \ll k_e, k_h$ ,  $\operatorname{sgn}(x)$  returns the sign of  $x$ , and  $\Gamma(x)$  is the Euler gamma function. Equation (20) gives the charge and spin susceptibilities for  $a = b$ , i.e.  $\chi_{aa}(\delta Q) \equiv \chi_{C/S,aa}(Q - 2k_a)$ , and the inter-pocket pair susceptibility for  $a \neq b$ , i.e.  $\chi_{eh}(\delta Q) \equiv -2\chi_{P,eh}(Q - Q_{eh}^+)$ ,  $Q_{eh}^+ = k_e + k_h$ . Equations (19) and (20) represent the main technical results of this work. We emphasize that they are valid only for  $D > 1$ . In the one-dimensional case, the dynamic screening is no longer irrelevant and qualitatively affects the scaling [44, 45].

For  $\gamma_{ab} < \gamma_c$  all susceptibilities in Eq. (20) are finite, supporting the FL ground state at weak coupling. However, at  $\gamma_{ab} > \gamma_c$  the susceptibilities in Eq. (20) are divergent at  $\delta Q = 0$ . Right at the quantum critical point when  $\gamma_{ab} = \gamma_c$ , the two-dimensional ( $D = 2$ ) susceptibilities feature a logarithmic divergence for small  $|\delta Q|$ ,  $\chi_{ab}(\delta Q) \propto \ln |\delta Q R_0|$ , see Fig. 3, while the three-dimensional ( $D = 3$ ) susceptibilities develop a finite jump at  $\delta Q = 0$ ,  $\chi_{ab}(\delta Q) \propto \operatorname{sgn}(\delta Q)$ , see Fig. S4 in the SM [47]. This behavior is striking and signals an instability of the FL towards the formation of the competing PDW, CDW, and SDW orders at  $\gamma_{ab} > \gamma_c$ , a behavior which is consistent with experimental observations in many strongly correlated electron systems [1–28]. We stress that the PDW instability found here requires the presence of both electron and hole Fermi surfaces, while the CDW and SDW instabilities emerge even within the

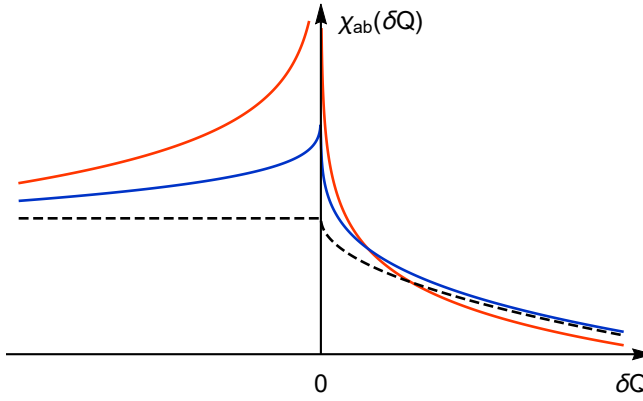


FIG. 3. **Susceptibility vs. momentum.**  $\chi_{ab}(\delta Q)$  as function of  $\delta Q = Q - (k_a + k_b) \ll 1/R_0 \ll k_a + k_b$  [see Eq. (20)], plotted for  $D = 2$  at different values of  $\gamma_{ab}$ : 1)  $\gamma_{ab} = 0$  (black dashed curve) corresponds to the well-known square-root anomaly for the free two-dimensional susceptibilities; 2)  $\gamma_{ab} = 0.25 = \gamma_c/2$  (blue curve) shows a sharp but finite peak near  $\delta Q = 0$ ; 3)  $\gamma_{ab} = 0.5 = \gamma_c$  (red curve) is logarithmically divergent at  $\delta Q = 0$ , which signals the  $Q = k_a + k_b$  instability.

single-pocket model. As our model is not material specific, this behavior is universal for all  $D$ -dimensional metals,  $D > 1$ , with a finite-range repulsive interaction. We note that strong interaction effects can be measured in the FL state at  $\gamma_{ab} < \gamma_c$  via local STM measurements of the charge and spin Friedel oscillations decaying via the anomalous power-law  $\propto 1/r^{D-\gamma_{ab}}$ .

*Discussion and future directions.* The two-pocket model of the PDW superconductivity presented in this work could be relevant to describe strong electron correlations in cuprate materials [1, 36–39]. In the overdoped FL state, cuprates feature a large Fermi surface, and the estimated Thomas-Fermi screening length for the Coulomb interaction is extremely short,  $R_0 \sim 1\text{\AA}$ . However, substantial experimental evidence points towards a potential Lifshitz transition, resulting in the reconstruction of the Fermi surface into a few small electron and hole pockets near the optimal doping in cuprates [3–6] where the PDW superconductivity as well as the CDW/SDW orders were observed [2–9], which lends support to our model. Such reconstruction of the Fermi surface in cuprates results in a dramatic reduction of the effective planar charge carrier density by one order of magnitude compared to the large-Fermi-surface FL state [3–6]. This strongly suppresses the Thomas-Fermi screening and results in much larger screening length which can exceed the average inter-electron distance. Therefore, we believe that all necessary conditions, such as the presence of both electron and hole pockets, as well as large enough screening lengths, exceeding the average inter-electron distance, could be met in high-temperature cuprate superconductors.

The superconducting order observed in MAG and double-bilayer graphene [19–24, 28] is also associated with a Lifshitz transition resulting in reconstructed

Fermi surfaces containing both electron and hole pockets [24, 34, 35]. This could potentially signal the PDW origin of superconductivity in these strongly correlated quantum materials as well. It might be possible to change the interaction range  $R_0$  in these materials in a controlled way by gates and thereby test our predictions.

In case of the single-pocket model, only the  $2k_F$  harmonics of charge and spin susceptibilities are singular at the critical coupling, signaling a phase transition from FL to a strongly correlated CDW/SDW insulator. We believe that this mechanism of metal-to-insulator transitions is relevant to experimental observations in ultraclean semiconductor quantum wells [10–13].

The mechanism of PDW, CDW, and SDW instabilities uncovered here is not material-specific but rather universal for interacting electron systems in dimensions  $D > 1$ . Therefore, our model and theory could also be relevant to experimental observations of quantum phase transitions in other materials [25–28].

In order to study the competition between PDW, CDW, and SDW orders, the inclusion of the corresponding condensates at  $\gamma_{ab} > \gamma_c$  is required. Melting of these orders at high temperatures could potentially describe the strange-metal state observed in strongly correlated electron systems. A detailed theoretical description of these effects is currently under way and left for a subsequent study.

*Conclusions.* We proposed and analyzed a realistic microscopic model universally describing all key features of high-temperature superconductors and correlated insulators observed in a large variety of quantum materials. In particular, we find a (logarithmic) singularity at finite momentum of the inter-pocket pair susceptibility and of the intra-pocket charge and spin susceptibilities at a critical universal value of the interaction coupling constant. This singularity signals a quantum phase transition from the FL to an ordered state described by competing PDW, CDW, and SDW orders which is consistent with the PDW scenario of superconductivity in cuprate materials [1, 36–39]. In the single-pocket model, only charge and spin susceptibilities feature a singularity at  $Q = 2k_F$  at the critical coupling, signaling a metal-to-insulator phase transition. Such a behavior is consistent with experimental observations in ultraclean semiconductor quantum wells at very low electron densities. Competition between the PDW, CDW, and SDW orders, as well as their melting and possible formation of the strange-metal state at high temperatures is deferred to a subsequent study.

*Acknowledgments.* We wish to acknowledge hospitality at The Anthony J. Leggett Institute for Condensed Matter Theory, Urbana (USA), during the inauguration workshop New Horizons in Condensed Matter Physics, November, 2023, which stimulated this work. This work was supported by the Georg H. Endress Foundation and the Swiss National Science Foundation (SNSF). This project has received funding from the European Union’s Horizon 2020 research and innovation programme under

Grant Agreement No. 862046.

---

[1] D. F. Agterberg, J. S. Davis, S. D. Edkins, E. Fradkin, D. J. Van Harlingen, S. A. Kivelson, P. A. Lee, L. Radzihovsky, J. M. Tranquada, and Y. Wang, *Annu. Rev. Condens. Matter Phys.* **11**, 231 (2020).

[2] T. Sato, T. Kamiyama, T. Takahashi, K. Kurahashi, and K. Yamada, *Science* **291**, 1517 (2001).

[3] N. Doiron-Leyraud, C. Proust, D. LeBoeuf, J. Levallois, J.-B. Bonnemaison, R. Liang, D. A. Bonn, W. N. Hardy, and L. Taillefer, *Nature* **447**, 565 (2007).

[4] T. Helm, M. V. Kartsovnik, M. Bartkowiak, N. Bittrner, M. Lambacher, A. Erb, J. Wosnitza, and R. Gross, *Phys. Rev. Lett.* **103**, 157002 (2009).

[5] H. Jang, S. Asano, M. Fujita, M. Hashimoto, D. H. Lu, C. A. Burns, C.-C. Kao, and J.-S. Lee, *Phys. Rev. X* **7**, 041066 (2017).

[6] Y. Li, W. Tabis, Y. Tang, G. Yu, J. Jaroszynski, N. Barišić, and M. Greven, *Sci. Adv.* **5**, eaap7349 (2019).

[7] P. Fournier, P. Mohanty, E. Maiser, S. Darzens, T. Venkatesan, C. J. Lobb, G. Czjzek, R. A. Webb, and R. L. Greene, *Phys. Rev. Lett.* **81**, 4720 (1998).

[8] M. Hücker, N. B. Christensen, A. T. Holmes, E. Blackburn, E. M. Forgan, R. Liang, D. A. Bonn, W. N. Hardy, O. Gutowski, M. V. Zimmermann, S. M. Hayden, and J. Chang, *Phys. Rev. B* **90**, 054514 (2014).

[9] Y. Sato, S. Kasahara, H. Murayama, Y. Kasahara, E.-G. Moon, T. Nishizaki, T. Loew, J. Porras, B. Keimer, T. Shibauchi, and Y. Matsuda, *Nat. Phys.* **13**, 1074 (2017).

[10] A. Mokashi, S. Li, B. Wen, S. V. Kravchenko, A. A. Shashkin, V. T. Dolgopolov, and M. P. Sarachik, *Phys. Rev. Lett.* **109**, 096405 (2012).

[11] M. S. Hossain, M. K. Ma, K. A. V. Rosales, Y. J. Chung, L. N. Pfeiffer, K. W. West, K. W. Baldwin, and M. Shayegan, *Proc. Natl. Acad. Sci. U.S.A.* **117**, 32244 (2020).

[12] M. Yu. Melnikov, A. A. Shashkin, V. T. Dolgopolov, A. Y. X. Zhu, S. V. Kravchenko, S.-H. Huang, and C. W. Liu, *Phys. Rev. B* **99**, 081106 (2019).

[13] A. A. Shashkin and S. V. Kravchenko, *Ann. Phys.* **435**, 168542 (2021).

[14] Y. Cao, V. Fatemi, A. Demir, S. Fang, S. L. Tomarken, J. Y. Luo, J. D. Sanchez-Yamagishi, K. Watanabe, T. Taniguchi, E. Kaxiras, R. C. Ashoori, and P. Jarillo-Herrero, *Nature* **556**, 80 (2018).

[15] A. L. Sharpe, E. J. Fox, A. W. Barnard, J. Finney, K. Watanabe, T. Taniguchi, M. A. Kastner, and D. Goldhaber-Gordon, *Science* **365**, 605 (2019).

[16] Y. Xie, B. Lian, B. Jäck, X. Liu, C.-L. Chiu, K. Watanabe, T. Taniguchi, B. A. Bernevig, and A. Yazdani, *Nature* **572**, 101 (2019).

[17] D. Wong, K. P. Nuckolls, M. Oh, B. Lian, Y. Xie, S. Jeon, K. Watanabe, T. Taniguchi, B. A. Bernevig, and A. Yazdani, *Nature* **582**, 198 (2020).

[18] Y. Jiang, X. Lai, K. Watanabe, T. Taniguchi, K. Haule, J. Mao, and E. Y. Andrei, *Nature* **573**, 91 (2019).

[19] X. Lu, P. Stepanov, W. Yang, M. Xie, M. A. Aamir, I. Das, C. Urgell, K. Watanabe, T. Taniguchi, G. Zhang, A. Bachtold, A. H. MacDonald, and D. K. Efetov, *Nature* **574**, 653 (2019).

[20] M. Yankowitz, S. Chen, H. Polshyn, Y. Zhang, K. Watanabe, T. Taniguchi, D. Graf, A. F. Young, and C. R. Dean, *Science* **363**, 1059 (2019).

[21] Y. Cao, V. Fatemi, S. Fang, K. Watanabe, T. Taniguchi, E. Kaxiras, and P. Jarillo-Herrero, *Nature* **556**, 43 (2018).

[22] M. Oh, K. P. Nuckolls, D. Wong, R. L. Lee, X. Liu, K. Watanabe, T. Taniguchi, and A. Yazdani, *Nature* **600**, 240 (2021).

[23] J. M. Park, Y. Cao, K. Watanabe, T. Taniguchi, and P. Jarillo-Herrero, *Nature* **590**, 249 (2021).

[24] H. S. Arora, R. Polski, Y. Zhang, A. Thomson, Y. Choi, H. Kim, Z. Lin, I. Z. Wilson, X. Xu, J.-H. Chu, K. Watanabe, T. Taniguchi, J. Alicea, and S. Nadj-Perge, *Nature* **583**, 379 (2020).

[25] L. Wang, E.-M. Shih, A. Ghiotto, L. Xian, D. A. Rhodes, C. Tan, M. Claassen, D. M. Kennes, Y. Bai, B. Kim, K. Watanabe, T. Taniguchi, X. Zhu, J. Hone, A. Rubio, A. N. Pasupathy, and C. R. Dean, *Nat. Mater.* **19**, 861 (2020).

[26] C. Shen, Y. Chu, Q. Wu, N. Li, S. Wang, Y. Zhao, J. Tang, J. Liu, J. Tian, K. Watanabe, T. Taniguchi, R. Yang, Z. Y. Meng, D. Shi, O. V. Yazyev, and G. Zhang, *Nat. Phys.* **16**, 520 (2020).

[27] P. Rickhaus, F. K. de Vries, J. Zhu, E. Portoles, G. Zheng, M. Masseroni, A. Kurzmann, T. Taniguchi, K. Watanabe, A. H. MacDonald, T. Ihn, and K. Ensslin, *Science* **373**, 1257 (2021).

[28] R. Su, M. Kuiiri, K. Watanabe, T. Taniguchi, and J. Folk, *Nat. Mater.* **22**, 1332 (2023).

[29] A. V. Chubukov, D. V. Efremov, and I. Eremin, *Phys. Rev. B* **78**, 134512 (2008).

[30] S. Raghu and S. A. Kivelson, *Phys. Rev. B* **83**, 094518 (2011).

[31] A. V. Chubukov, M. Khodas, and R. M. Fernandes, *Phys. Rev. X* **6**, 041045 (2016).

[32] S.-S. Lee, P. A. Lee, and T. Senthil, *Phys. Rev. Lett.* **98**, 067006 (2007).

[33] H. Isobe, N. F. Q. Yuan, and L. Fu, *Phys. Rev. X* **8**, 041041 (2018).

[34] E. Laksono, J. N. Leaw, A. Reaves, M. Singh, X. Wang, S. Adam, and X. Gu, *Solid State Commun.* **282**, 38 (2018).

[35] C.-C. Liu, L.-D. Zhang, W.-Q. Chen, and F. Yang, *Phys. Rev. Lett.* **121**, 217001 (2018).

[36] E. Berg, E. Fradkin, and S. A. Kivelson, *Nature Phys* **5**, 830 (2009).

[37] E. Berg, E. Fradkin, S. A. Kivelson, and J. M. Tranquada, *New J. Phys.* **11**, 115004 (2009).

[38] D. F. Agterberg and J. Garaud, *Phys. Rev. B* **91**, 104512 (2015).

[39] Y. Wang, S. D. Edkins, M. H. Hamidian, J. C. S. Davis, E. Fradkin, and S. A. Kivelson, *Phys. Rev. B* **97**, 174510 (2018).

[40] J. Hutchinson, D. Miserev, J. Klinovaja, and D. Loss, ArXiv:2310.05555, [2310.05555 \[cond-mat\]](https://arxiv.org/abs/2310.05555).

[41] S. Gangadharaiah, D. L. Maslov, A. V. Chubukov, and

L. I. Glazman, *Phys. Rev. Lett.* **94**, 156407 (2005).

[42] D. L. Maslov and A. V. Chubukov, *Phys. Rev. B* **79**, 075112 (2009).

[43] R. A. Žak, D. L. Maslov, and D. Loss, *Phys. Rev. B* **85**, 115424 (2012).

[44] N. Menyhard and J. Sólyom, *J. Low Temp. Phys.* **12**, 529 (1973).

[45] J. Sólyom, *J. Low Temp. Phys.* **12**, 547 (1973).

[46] D. Miserev, J. Klinovaja, and D. Loss, *Phys. Rev. B* **108**, 235116 (2023).

[47] See Supplemental Material at ... where we present technical details for first- and second-order perturbation theory, renormalization group construction,  $D$ -dimensional Fourier transforms, and plot of three-dimensional susceptibility given by Eq. (20) in the main text.